J Solid State Eletrochem (2004) 8: 450–466
DOI 10.1007/s10008-004-0521-1

REVIEW

H. Liu · Y. P. Wu · E. Rahm · R. Holze · H. Q. Wu

# Cathode materials for lithium ion batteries prepared by sol-gel methods

Received: 7 May 2003 / Accepted: 13 February 2004 / Published online: 27 March 2004


**Abstract** Improving the preparation technology and electrochemical performance of cathode materials for lithium ion batteries is a current major focus of research and development in the areas of materials, power sources and chemistry. Sol-gel methods are promising candidates to prepare cathode materials owing to their evident advantages over traditional methods. In this paper, the latest progress on the preparation of cathode materials such as lithium cobalt oxides, lithium nickel oxides, lithium manganese oxides, vanadium oxides and other compounds by sol-gel methods is reviewed, and further directions are pointed out. The prepared products provide better electrochemical performance, including reversible capacity, cycling behavior and rate capability in comparison with those from traditional solid-state reactions. The main reasons are due to the following several factors: homogeneous mixing at the atomic or molecular level, lower synthesis temperature, shorter heating time, better crystallinity, uniform particle distribution and smaller particle size at the nanometer level. As a result, the structural stability of the cathode materials and lithium intercalation and deintercalation behavior are much improved. These methods can also be used to prepare novel types of cathode materials such as nanowires of $LiCoO_2$ and nanotubes of $V_2O_5$, which cannot be easily obtained by traditional methods. With further development and application of sol-gel methods, better and new cathode materials will become available and the advance of lithium ion batteries will be greatly promoted.

H. Liu · Y. P. Wu (✉) · H. Q. Wu
Department of Chemistry & Shanghai Key Laboratory of Molecular Catalysis and Innovative Materials, Fudan University, 200433 Shanghai, China
E-mail: wuyp@fudan.edu.cn

Y. P. Wu · E. Rahm · R. Holze (✉)
Institut für Chemie, AG Elektrochemie, Technische Universität Chemnitz, 09111 Chemnitz, Germany
E-mail: rudolf.holze@chemie.tu-chemnitz.de

**Keywords** Cathode materials · Lithium ion battery · Sol-gel method · Doping · Coating

## Introduction

Stimulated by the first oil crisis in the middle of the 1970s, the need for high-energy power sources for light electronics, environmental protection from the use of poisonous Pb and Cd and better utilization of natural sources, a breakthrough in the commercialization of the lithium ion battery was finally achieved in the late 1980s and early 1990s. It was found that lithium metal or alloys could be substituted by graphitic carbon, and the safety problem associated with cycling was completely solved. Since the lithium ion battery presents many advantages over the traditional rechargeable systems such as lead acid and Ni-Cd, its development has been very rapid, although it is more expensive, and now it has been widely applied in many light electronics with high value such as portable telephones and computers, digital cameras and video cameras [1].

Current research on cathode materials for lithium ion batteries is very active and many preparation methods have been widely explored, such as incorporation of heteroatoms [2], composite technology [3, 4], soft-chemistry routes including ion exchange, hydrothermal and oxidation–reduction reactions [5, 6], some non-classical methods such as mechano-chemical methods, template methods, pulsed laser deposition, plasma-enhanced chemical vapor deposition, radiofrequency magnetron sputtering [7] and sol-gel methods. Among them, sol-gel methods are promising since they have many advantages over conventional solid-state reactions such as homogeneous mixing at the atomic or molecular level, good stoichiometric control, low synthesis temperature, short heating time, good crystallinity, uniform particle size and small diameter, even at the nanometer level [8, 9].

The beginning of the sol-gel methods can be dated back to as early as 1846 when Ebelenen [1] discovered

the formation of $SiO_2$ gel by hydrolyzing $Si(OEt)_4$. Only in the 1930s did this method begin its further development. The basic processing steps of this method can be summarized as follows:

Precursor → hydrolysis → reactive monomer → condensation → sol gelation → gel → further treatment.

On the basis of this synthetic route, variations of precursors, solvents, ligands, different addition sequences of compounds, further treatment and other changes in sol-gel methods have been reported and widely applied in the preparation of, for example, glasses, ceramics, inorganic fillers and coatings [8, 9, 10]. As mentioned above, after the commercialization of lithium ion batteries in the early 1990s, sol-gel methods were employed to prepare materials for this energy conversion and storage system. In this paper, recent progress in the preparation of cathode materials by sol-gel methods is reviewed, including lithium cobalt oxides ($LiCoO_2$), lithium nickel oxides ($LiNiO_2$), lithium manganese oxides ($LiMn_2O_4$), vanadium oxides and other materials, and further developmental directions are pointed out.

## Lithium cobalt oxides

$LiCoO_2$ prepared at high temperatures has a layered structure like $\alpha$-$NaFeO_2$, based on a closely packed network of oxygen atoms with $Li^+$ and $Co^{3+}$ ions located on alternating (111) planes of the cubic rock-salt structure. It is superior in cycling behavior due to its high structural stability and can be cycled more than 500 times with 80–90% capacity retention [1]. As a result, it is the most common cathode material besides $LiNiO_2$, $LiMn_2O_4$ and vanadium oxides on the market. Usually, $LiCoO_2$ is prepared by a solid-state reaction, i.e. heat treating the mixture of the solid lithium salt such as $LiNO_3$, LiOAc, $Li_2CO_3$ or LiOH and oxides of cobalt such as $Co_3O_4$ and $Co_2O_3$ or cobalt salts such as $Co(NO_3)_2$ and $Co(OAc)_2$. This kind of reaction needs a long heating time and high temperature to obtain uniform and good products since the diffusion coefficient of $Li^+$ ions is not high. In order to overcome this shortcoming, sol-gel methods are preferred, and they can be used to prepare lithium cobalt oxides, both doped and coated.

### Lithium cobalt oxides prepared by sol-gel methods

A general sol-gel method used to prepare $LiCoO_2$ is as follows. A cobalt salt is dissolved in water and the pH is adjusted with LiOH and aqueous ammonium solution to form a gel. During this process, the control of the pH is very important. If it is not well controlled, precipitation will happen, and thus it is sometime called the co-precipitation method [1].

In order to control the particle size and uniformity of the products, an organic acid can be added as a carrier. In order that the interaction (complexing) between the metal ions and polar side groups ensures homogeneous distribution of the constituent ions and enhances the crystallization process during the following heat treatment, the carrier should have hydrophilic functional groups such as hydroxides or carboxylates, which include small molecules like succinic acid, oxalic acid, malic acid, tartaric acid, acrylic acid, citric acid, humic acid and polymers like poly(acrylic acid) (PAA) and poly(vinylpyrrolidone) (PVP) [1, 11, 12, 13, 14, 15, 16, 17, 18, 19].

With PAA as an example, a preparation procedure is shown in Scheme 1 [15]. At first, aqueous solutions of the lithium and cobalt salts are mixed with an aqueous solution of PAA using nitric acid to fix the pH at 1–2. After evaporation at 70–80 °C, a transparent pink sol is obtained. Further evaporation makes the sol change to a viscous transparent pink gel. Then the gel precursor is heated at 300 °C to eliminate the organic components to obtain a precursor powder. Single-phase polycrystalline $LiCoO_2$ is prepared after heat treatment of this powder at 400–800 °C. The ratio of PAA to metal ions can be changed, but it should be enough to suppress cation mobility during the heat treatment. Excess or too small a ratio should be avoided. With an excess, the partial pressure of $O_2$ will be too low, and the complete oxidation of $Co^{2+}$ to $Co^{3+}$ will be prevented. If it is too small, it will be similar to the solid-state reaction, and

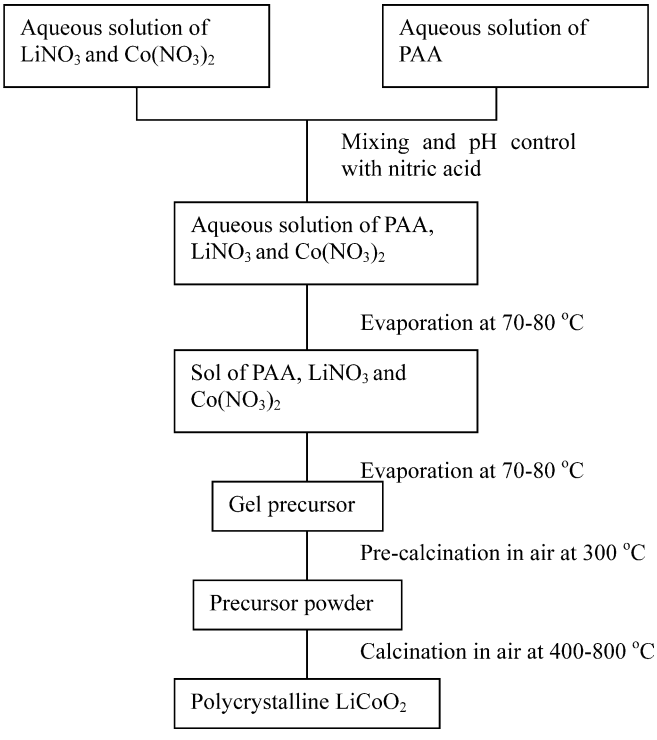


**Scheme 1** Preparation procedure of polycrystalline $LiCoO_2$ by a sol-gel method using poly(acrylic acid) as complexing agent (modified from [16])

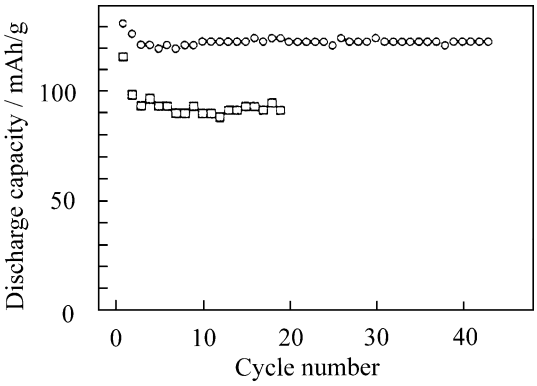


**Fig. 1** Comparison of the cycling behavior of $LiCoO_2$ prepared by sol-gel methods (*open circles*) and traditional solid-phase methods (*open squares*) (from [9])

the advantages of the sol-gel method would not be displayed.

During the process of formation of the gel, owing to the combination of cobalt and lithium ions with oxygen atoms of the acid, not only can the size of the particles be controlled at the nanometer level (in the range of 30–50 nm) and the specific BET surface area in the range of 2.3–17 $m^2/g$, but also the mixing can be completely uniform at an atomic level. $LiCoO_2$ with good crystallinity can be prepared at a relatively low temperature. In addition, long-time heating required by solid-state reactions is not needed. Both the reversible capacity and cycling behavior of the obtained $LiCoO_2$ are superior to those from the solid-state reaction. The reversible capacity can be above 150 mAh/g as compared to 120 mAh/g obtained with the solid-state reaction product. Figure 1 shows an example of this comparison when cycled with lithium metal as reference electrode, and 97% of the initial discharge capacity after 350 cycles is still retained [16]. By the way, the sol-gel method can be used to prepare thin-film electrodes, which cannot be easily realized by solid-state reactions [19].

However, it is also reported that $LiCoO_2$ synthesized at low temperature has an intermediate structure between a layered and spinel structure, whose reversible capacity is low, about 80 mAh/g. This result shows that heat treatment at a high temperature is still necessary to obtain a good and stable layered structure [14], but the time will be much shorter in comparison with that for the solid-state reaction.

Condensation polymers, such as that from ethylene glycol and citric acid, can also be used as carriers for $Li^+$ and $Co^{3+}$ ions if they have hydrophilic functional groups such as hydroxides or carboxylates, which can combine with the cations to ensure their mixing at the atomic level [20]. In addition, when an anodic aluminum oxide template is dipped in a sol comprising LiOAc, $Co(OAc)_2$ and a condensation polymer of citric acid and ethylene glycol, after heat treatment of the sol at a high temperature, nanowires of $LiCoO_2$ with highly ordered arrays and a uniform length and diameter can be prepared [21].

## Doped lithium cobalt oxides prepared by sol-gel methods

Since the cost of Co is the highest among Co, Ni, Mn and V, its application is only limited to high-value products such as video devices, cameras and portable computers [1]. Consequently, heteroatoms are introduced to lower the cost and/or improve the electrochemical performance [2]. The introduction of heteroatoms can also be performed by sol-gel methods. For example, Al-doped $LiCoO_2$ can be prepared by using acrylic acid as a carrier for a sol-gel method [22, 23]. The composite shows a well-developed layered $\alpha$-$NaFeO_2$ structure when it is prepared at 600 °C or higher [22]. When the heat-treatment temperature is decreased, the capacity fading of the doped $LiCoO_2$ is greatly reduced. After partial substitution, there is an increase in the peak temperature in DSC measurements and a reduction in the exothermic peak as compared to undoped material. This indicates that Al-doped $LiCoO_2$ has good thermal stability [23], which provides a promising direction in improving the thermal behavior of lithium ion batteries, especially in the application as power sources for electric vehicles since safety problems associated with thermal production are the main concerns for large batteries.

Other kinds of favorable heteroatoms can also be taken into consideration to prepare doped $LiCoO_2$ with good electrochemical performance by sol-gel methods [2].

## Coated lithium cobalt oxides prepared by sol-gel methods

As mentioned above, the structural stability of $LiCoO_2$ is the highest among the current cathode materials. However, in case of the application of these materials at higher operating temperatures or in space exploration, much improvement is still needed [1]. Coating oxides by sol-gel methods is a promising choice [24, 25], and the coating process, using $Al_2O_3$ for an example, is performed as follows [24]:

$$\text{Hydrolysis:}\quad Al(OR)_3 + H_2O \rightarrow Al(OR)_2(OH) + ROH \tag{1}$$

$$\text{Polycondensation:}\quad Al(OR)_2(OH) + Al(OR)_2(OH) \rightarrow (OR)_2Al\text{ - }O\text{ - }Al(OR)_2 + H_2O \tag{2}$$

$$\text{Particle surface - OH} + (OR)Al(OR)_2 \rightarrow \text{particle surface - O - } Al(OR)_2 + ROH \tag{3}$$

Accordingly, Al-OR groups react with $LiCoO_2$ surface-OH groups, resulting in good adhesion of aluminum oxide gel to the surface of $LiCoO_2$ particles, according to Eq. 3. After the subsequent heat treatment, $Al_2O_3$-coated $LiCoO_2$ is obtained, which does not

contain any $Al_2O_3$ phase. During cycling there is no phase transition from a hexagonal to a monoclinic phase at 4.15–4.2 V. The disappearance of such a phase transition accompanied by improved layer characteristics in cation order improves the capacity retention of the cathode [24]. The main reason is that a solid solution $LiCo_{1-x}Al_xO_2$ is present on the surface of $LiCoO_2$ as a coating. Other kinds of oxides such as $SnO_2$ can also be coated on the surface of $LiCoO_2$ by sol-gel methods, and excellent structural stability, disappearance of the phase transition, improved capacity retaining and tolerance to overcharge are achieved [25].

It should be noted that the distribution of this coating can yield different results. When this coating is beyond 50 nm or distributed throughout the host material, no evident improvement has been observed. The heat-treatment temperature (HTT) can affect the distribution of the coating, and it seems that its transitional value depends on the coating species. In the case of $Al_2O_3$ coating, when the HTT is below 700 °C, the solid solution $LiCo_{1-x}Al_xO_2$ mainly exists on the surface of $LiCoO_2$ particles within 50 nm [24]. If higher, then it will beyond 50 nm. In the case of $SnO_2$, when the HTT is below 600 °C, Sn is mainly distributed on the surface. In contrast, when the HTT is 600 °C, Sn distributes uniformly throughout the coated $LiCoO_2$ particles [25].

These results demonstrate the advantages of the sol-gel method in the preparation of $LiCoO_2$ cathode materials, such as shorter heat-treatment time, better crystallinity, uniform particle size, higher capacity and better structural stability. Doping and coating will decrease the cost and improve the structural stability and the resulting cycling behavior. With the development of lithium ion battery technology, combinations of the sol-gel method with other methods such as doping [2] or composite material formation [4] will promote the electrochemical performance and lower the cost. Additional fields of application might be accessible and new kinds of $LiCoO_2$ cathode materials such as 5 V cathode materials will be available.

## Lithium nickel oxides

$LiNiO_2$ has a layered structure similar to $LiCoO_2$. Although it is cheaper than $LiCoO_2$ and its reversible capacity is higher than that of $LiCoO_2$, it is difficult to prepare on a large scale with an ideal layered structure. The main reason is the difficult oxidation of $Ni^{2+}$ to $Ni^{3+}$. In addition, $LiNiO_2$ decomposes easily into Li-deficient compounds, $Li_dNiO_{2-d}$ ($0 < d < 1$), when prepared at high temperature, which act as phase impurities and are unfavorable for lithium intercalation and deintercalation. In order to overcome these disadvantages for synthesis, sol-gel methods are preferred as with $LiCoO_2$ since the preparation temperature and the heat-treatment time can be decreased to obtain crystalline $LiNiO_2$ with fewer phase impurities [1, 11, 16, 18, 22, 26, 27, 28, 29, 30].

### Lithium nickel oxides prepared by sol-gel methods

The general process of the sol-gel method is similar to that for the preparation of $LiCoO_2$ [26]. At first, lithium hydroxide and ammonium hydroxide are added to a nickel salt solution of, for example, nickel nitrate. After obtaining a gelatinous precipitate, the solvents are removed by evaporation at temperatures below 100 °C. Then, the unreacted lithium compounds are removed by washing with water. The resulting dried powder is heat treated at a temperature above 400 °C to obtain crystalline $LiNiO_2$ [26].

Organic carriers such as small molecules like citric acid [18, 27], adipic acid [28] and polymers like poly(-vinyl alcohol) [29] or poly(vinylbutyral) [30] can also be added to prepare $LiNiO_2$ since they can form complexes with cations of $Li^+$ and $Ni^{2+}$. For example, in the case of citric acid, complexes of $LiNi(C_6H_4O_7)_{3/4}{\cdot}xH_2O$, $LiNi(C_6H_5O_7){\cdot}xH_2O$ and $(NH_4)_3LiNi(C_6H_5O_7)_2{\cdot}xH_2O$ ($x \approx 5$) have been detected by freeze drying of concentrated lithium–nickel–citrate solutions [18]. As a result, the homogeneous distribution of the constituent ions favors easy crystallization during heat treatment.

In comparison with samples obtained from solid-state reactions, the crystalline $LiNiO_2$ prepared by the above sol-gel methods displays good capacity retention. For example, after 350 cycles more than 90% of the initial capacity is retained [26]. One of the reasons is that the mixing of Li and Ni is homogeneous at the atomic level, and thus crystalline $LiNiO_2$ can be prepared at a lower temperature with a shorter time to avoid the appearance of impure phases from the decomposition of $LiNiO_2$, and the particle size is smaller. Another reason is perhaps that an additional heat released by oxidation of the organic carriers during the heat treatment accelerates the formation of $LiNiO_2$ crystals. As a result, the disordering or the mixing of cations of $Ni^{3+}$ and $Li^+$ ions is greatly reduced, the chemical diffusivity of $Li^+$ is increased, the instantaneous internal resistance (IR) during the first intermittent discharge is decreased, and the reversibility and the rate capability are improved.

An excess of organic carrier is not desirable, since its oxidation will cause the partial pressure of $O_2$ to be too low and affect the complete oxidation of $Ni^{2+}$ to $Ni^{3+}$. Nanometer $LiNiO_2$ can be stable up to 400 °C, and the initial reversible capacity is 150 mAh/g [26].

### Doped lithium nickel oxides prepared by sol-gel methods

In order to inhibit the reduction of $Ni^{4+}$ during cycling, doping with heteroatoms such as Al, Co or Li can also be employed to stabilize $LiNiO_2$ and to improve the electrochemical performance; this can be carried out based on sol-gel methods [2, 31, 32, 33, 34, 35, 36, 37, 38]. For example, the preparation of $LiAl_yNi_{1-y}O_2$ ($y = 0$–$0.3$) is similar to Scheme 1 except that adipic acid

as the carrier and acetic acid as the pH controlling agent ($2.5 < pH < 3.5$) are used [32]. Since the bond energy of Al–O (512 kJ/mol) is higher than that of Ni–O (391.6 kJ/mol), the stability of the $LiNiO_2$ structure is enhanced and the obtained $LiAl_yNi_{1-y}O_2$ displays good cycling performance even at a high temperature (50 °C) [32]. Among the $LiNi_{1-y}Al_yO_2$ ($y = 0$, 0.05, 0.1, 0.2, 0.25, 0.3) samples, $LiNi_{0.95}Al_{0.05}O_2$ has the best electrochemical properties, with a relatively large first discharge capacity and an excellent cycling performance [38].

Cobalt doping into $LiNiO_2$ can be performed by sol-gel methods and the carriers can also include small molecules such as maleic acid and citric acid [33, 34, 35] and polymers such as poly(ethylene alcohol) [39]. Good crystalline $LiNi_{1-y}Co_yO_2$ can also be prepared at a low HTT such as 600 °C [39], and the doping amount of Co can be adjusted. A $y$ value of 0.25 in $LiNi_{1-y}Co_yO_2$ shows the largest initial discharge capacity and the best cycling performance [37]. Synthesis conditions such as the solvent, the calcination time and temperature, the ratio of acid to metal ions, and the lithium stoichiometry can affect the electrochemical performance of the prepared $LiNi_{0.8}Co_{0.2}O_2$ [33, 34]. The solvent can affect the initial formation of a chelating complex, which decides the homogeneity of the final compound. Increase of the ratio of acid to metal ions above 1 will lead to a lack of hexagonal ordering and a corresponding decrease in capacity [33]. The calcination time and temperature influence the lattice parameters and the amount of Ni in the Li 3a site [34]. One optimal synthesis condition has been found with ethanol as solvent and a calcination time of 12 h at 800 °C under flowing oxygen [33]. The first discharge capacity of the material synthesized using these conditions is 190 mAh/g, and the discharge capacity after 10 cycles is 183 mAh/g at a 0.1 C rate between 3.0 and 4.2 V vs. $Li^+/Li$ (in the following text, potentials are referred to $Li^+/Li$ if not indicated otherwise) [33]. This good performance resulted from better hexagonal ordering, crystallinity and smaller particle size with good particle-size distribution [37]. The ratio of maleic acid to metal ions also influences the electrochemical performance. When it is above 1, it will lead to a lack of hexagonal ordering and a corresponding decrease in capacity [33].

On the basis of the cobalt-doped $LiNiO_2$, further doping can also be performed by the sol-gel method. For example, using oxalic acid as a carrier, $LiSr_xCo_{0.2}Ni_{0.8}$ can be prepared [41]. When $x$ is $10^{-6}$, an improved capacity and cyclability with a first cycle discharge capacity of 173 mAh/g and a 10th cycle capacity of 167 mAh/g have been achieved. However, when $x$ is above $10^{-4}$, there is a sharp decrease in the discharge capacity. As to the detailed actions, further study is needed.

Precursors for $LiNiO_2$ can also be prepared by sol-gel methods and good results can also be achieved [31]. For example, when using spherical $Ni_{1-x}Co_x(OH)_2$ ($x = 0.1$, 0.2 or 0.3) powder from a sol-gel method as a precursor to prepare $LiNi_{1-x}Co_xO_2$, its crystal parameter ratio $c/a$, electrochemical stability and density are increased in combination with an increase in the volumetric capacity because of the lowered cation disordering in comparison with the prepared $Li_{1-x}Co_xNi_{1-x}O_2$ obtained by mixing of $Co(OH)_2$ and $Ni(OH)_2$ with subsequent heat treatment [31]. With an increase in x, the ratio $c/a$ and electrochemical stability also increase. The reversible capacity of $LiNi_{0.75}Co_{0.25}O_2$ can be up to 182 mAh/g [40].

On the basis of $LiNi_{1-y}Co_yO_2$, an excess of lithium can also be doped by sol-gel methods [36, 37]. Excess lithium stoichiometry showed interesting properties, such as improved capacity and cyclability. Of all the compositions with excess lithium stoichiometry, $Li_{1.1}Ni_{0.8}Co_{0.2}O_2$ shows electrochemical characteristics with a first cycle discharge capacity of 182 mAh/g and in the 10th cycle 172 mAh/g, better than the ideal stoichiometry $LiNi_{0.8}Co_{0.2}O_2$. Excess lithium stoichiometry will saturate the lithium sites, preventing the movement of transition metal ions into any unoccupied sites such as the change of $Ni^{2+}$ ions at lithium sites [37]. However, too large an excess of lithium should be avoided since lithium may occupy sites that are not suitable for the intercalation and deintercalation process and may result in adverse effects [36].

Other kinds of heteroatoms can be doped by sol-gel methods. However, it should be noted that the dopants will themselves cause favorable effects such as substituting $Ni^{2+}$ in the impure phase and inhibiting side actions from $Ni^{2+}$, forming inert layered $LiMO_2$ to substitute part of the $LiNiO_2$ and to prevent destruction of the $LiNiO_2$ structure from over-charge, increasing the stability of the crystal structure to circumvent phase transformation, decreasing the charge transfer resistance and increasing the $Li^+$ diffusion coefficient, and blocking $Ni^{2+}$ from diffusing into a $Li^+$ site [2].

## Coated lithium nickel oxides prepared by sol-gel methods

The phase transitions in $Li_{1-x}NiO_2$ when $x > 0.5$, for example from the original hexagonal phase (H1) to a monoclinic one (M), from M to another hexagonal phase (H2), or from H2 to the third hexagonal phase (H3), are very serious and produce detrimental effects (especially the latter two). As a result, microcracks are formed in each particle, induced by anisotropic lattice changes along the $a$ and $c$ axes in the initial hexagonal phase, and the capacity fades markedly with cycling. In order to circumvent this problem, it has been found that coating by a sol-gel method is a good choice. For example, a thin film of $ZrO_2$ using a sol-gel method can be coated on $LiNiO_2$ by the following process: Zr ethylhexanoisopropoxide $\{[Zr(OOC_8H_{15})_2(OC_3H_7)_2]\}$ is dissolved in isopropanol to obtain a gel, and then $LiNiO_2$ powder is added by mechanical mixing with mortar and pestle, followed by aging at 50 °C for 24 h

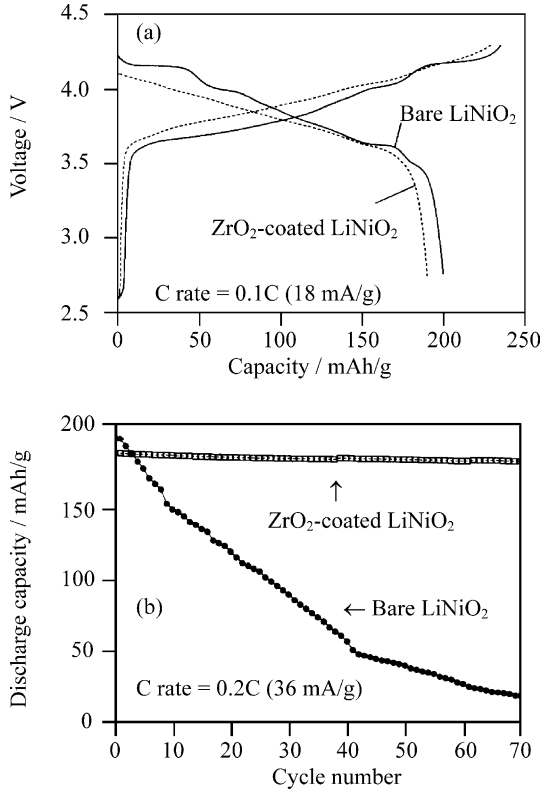


**Fig. 2** Charge and discharge profiles of bare and $ZrO_2$-coated $LiNiO_2$ in the first cycle between 4.3 and 2.75 V (**a**) at a rate of 0.1 C (18 mA/g) and (**b**) their cycling behavior at a rate of 0.2 C (36 mA/g) (from [42])

to ensure strong bonding between the gel and $LiNiO_2$ particles [42]. The $ZrO_2$-coated $LiNiO_2$ can effectively suppress lattice distortion and the consequent phase transition. As a result, the cycling performance is greatly improved, with only 2% capacity loss after 70 cycles when cycling between 4.3 and 2.75 V, as shown in Fig. 2 [42]. Other kinds of oxides can be coated by sol-gel methods, but one thing should be taken into consideration, namely that the coating should be situated at the surface of the $LiNiO_2$ particles. If it is on the inner side, the coating effects will disappear. This process can be controlled by the HTT, which should not be higher than a particular value, depending on the coating species.

The above results show that sol-gel methods can overcome the common problem encountered by solid-state reactions, i.e. the production of an impure phase and the disordering or mixing of $Li^+$ and $Ni^{2+}$, and thus $LiNiO_2$ prepared by sol-gel methods shows high stability. The introduction of heteroatoms and coating can further improve the stability and prevent the appearance of phase transformations. Consequently, its practical application in lithium ion batteries will not be a problem. By the way, the coating may provide a chance for higher voltage (5 V) applications since the contact between $Ni^{4+}$ and the electrolytes is effectively prevented.

## Lithium manganese oxides

There are various kinds of lithium manganese oxides [43]. Here we focus on the spinel $LiMn_2O_4$, whose structure is different from the previous layered cathode materials, $LiCoO_2$ and $LiNiO_2$. Since it is cheap and has low environmental impact, it is fairly attractive especially for application in electric vehicles. However, its capacity fades slowly, and this prevents its wide commercial use. This fading is mainly due to the following three factors:

1. Dissolution of $Mn^{3+}$. At the end of discharge, the concentration of $Mn^{3+}$ arrives at its highest level. The $Mn^{3+}$ at the surface may disproportionate according to Eq. 4 [1, 43, 44, 45, 46, 47, 48]:

$$2Mn^{3+}_{solid} \rightarrow Mn^{4+}_{solid} + Mn^{2+}_{solution} \quad (4)$$

   $Mn^{2+}$ ions from this disproportionation dissolve in electrolyte solutions.
2. The Jahn–Teller effect. At the end of discharge, the Jahn–Teller effect, happening at first on the surface of several particles, may expand into the overall composition of $Li_{1+\delta}[Mn_2]O_4$. This system is not really at a thermodynamic equilibrium [45, 47]. The phase transition from cubic to tetragonal symmetry is a first-order process. Even though this kind of change is small, it is laarge enough to destroy the structure to form a tetrahedral structure, which is low in symmetry and high in disorder [49].
3. In organic solvents, the highly delithiated particles are not stable at the end of the discharge, viz. the high oxidation capability of $Mn^{4+}$ leads to decomposition of the solvents [47, 50, 51].

These factors may act jointly, resulting in the capacity fading. In addition, the spinel $LiMn_2O_4$ from solid-state reactions usually contains some phase impurities, which are detrimental to the electrochemical performance. In order to overcome or partly alleviate this serious problem, one effective solution is the use of sol-gel methods since materials prepared in this way have few impurities, a small particle size with a homogeneous size distribution and a controlled morphology, in contrast to the traditional solid-state reaction.

### Lithium manganese oxides prepared by sol-gel methods

Thin film $LiMn_2O_4$ electrodes can be prepared by a sol-gel method using spin coating and annealing processes with anhydrous $Mn(CH_3COCHCOCH_3)_3$ (manganese acetylacetonate) and $Li(CH_3COCHCOCH_3)$ (lithium acetylacetonate) as precursors. Electrochemical properties of the film electrode depend on the drying temperature, even when subjected to the same annealing conditions. The discharge capacity of the annealed film

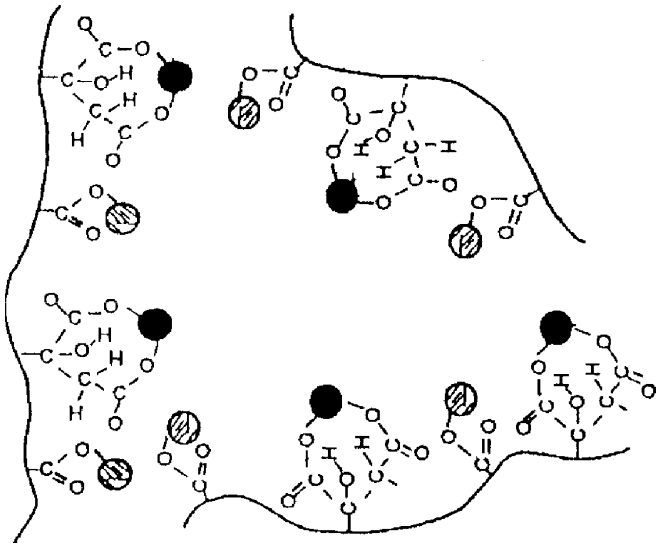

**Fig. 3** Schematic structure of the stable bulky glass of the condensation polymer of ethylene glycol and citric acid with $Mn^{2+}$ (*solid circles*) and $Li^{+}$ (*hatched circles*) (from [53])

increases with the drying temperature. However, the rate of capacity fading during cycling also increases with the drying temperature [52].

Polymeric carriers are also used for sol-gel methods, and there is little difference in the process depending on the polymers used. For example, the process using the condensation polymer of citric acid and ethylene glycol as a carrier is as follows [1, 44, 53, 54]. Nitrates of Mn and Li are at first dissolved in an aqueous solution of citric acid and ethylene glycol and partially neutralized to form a complex of citric acid with metal ions [53, 54]. Then the mixture is heated to esterify to form oligomers. With progress of the esterification the viscosity increases gradually, and this ensures the homogenous distribution of cations in the complex. A subsequent condensation process will remove the additional ethylene glycol to form a bulky glass. This glass is very stable and its structure is schematically illustrated in Fig. 3 [53]. Finally, the mixture is heat treated to prepare the spinel $LiMn_2O_4$. Prior to the heat treatment, the polymeric carrier is very stable, and there is no precipitation; $Li^{+}$ and $Mn^{3+}$ ions are homogeneously distributed in the polymeric supporter at the atomic level owing to coordination with the functional oxygen in the polymers [54]. If a condensation polymer containing hydrophilic groups such as poly(ethylene glycol) [55] and a radical polymer such as poly(acrylic acid) (PAA) or poly(vinylpyrrolidone) (PVP) [1, 19, 56] are directly used, the condensation process is not required. The carboxylic groups of PAA and the carbonyl groups of PVP form complexes with the added cations, producing a sol and resulting in the dispersion of cations in the polymeric carrier at an atomic level [56].

The structure of the obtained gel will change with the ratio of the carriers to the $Li^{+}$ and $Mn^{3+}$ ions [56], and it can be crosslinked or non-crosslinked. Usually an excess of the polymer carrier is used to form a crosslinked structure. As a result, there will be no dissipation during the heat treatment. Since long-range diffusion is not required for these sol-gel methods, unlike the solid-state reaction, a single spinel phase of $LiMn_2O_4$ can be obtained at a low temperature such as 250–300 °C [53, 56].

The electrochemical performance of the prepared $LiMn_2O_4$ is much improved in comparison with that from the solid-state reaction [53, 56]. For example, the reversible capacity is up to 135 mAh/g (91% of theoretical capacity) and the capacity fading is very slow. With lithium metal as a reference electrode, after 168 cycles the capacity fades only 9.5%, as shown in Fig. 4 [56].

Small molecules can be used as carriers to prepare $LiMn_2O_4$ by sol-gel methods. When adipic acid is used as a carrier, the performance of the obtained $LiMn_2O_4$ is better [57], especially when cycling at low temperature. The performance of the obtained $LiMn_2O_4$ using hydroxyacetic acid as a carrier can be comparable with that from the above-mentioned condensation polymer of citric acid and ethylene glycol. Its initial capacity is 134 mAh/g when the obtained $LiMn_2O_4$ is cycled between 3.6 and 4.3 V. It will retain 94% after 100 cycles [58, 59]. Butanedioic acid and citric acid can also be used as carriers [48, 60, 61, 62], and different conditions for the preparation, such as the pH, the molar ratio of carrier to total metal ion, the amount of water, the calcination temperature and the starting materials can affect the purity of this oxide. In the case of the pH, it

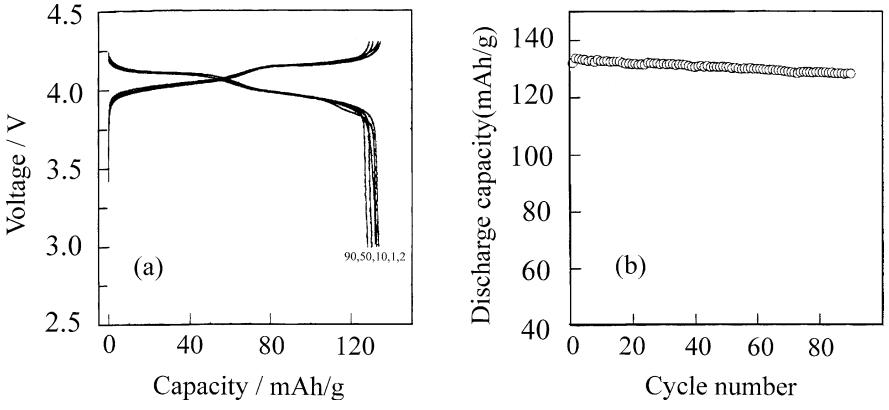


**Fig. 4** Electrochemical properties of the nanometer spinel $LiMn_2O_4$ synthesized by sol-gel methods using poly(acrylic acid) as a carrier: (**a**) charge and discharge curves at different cycles; (**b**) cycling behavior (from [56])

can affect the solubility of LiOH, the carrier and $Mn^{2+}$. When it is below 6.0, the solubility of the organic carrier will be low, and LiOH will be soluble in aqueous solution. When it is greater than 10.0, the organic carrier will be soluble in aqueous solution, $Mn^{2+}$ and $Li^{+}$ will be precipitated, and a stable complex will not be formed. When the molar ratio is below 1.0, segregation of the cations occurs and the combustion heat will be insufficient for the synthesis of $LiMn_2O_4$. If it is larger than 1.0, the temperature will be raised very high in a short period of time, leading to a decrease of the oxygen partial pressure and the formation of an impure phase of $Mn_2O_3$. The amount of water should not be too high since some cations can dissolve therein, resulting in the formation of lithium and manganese oxides, unfavorable for electrochemical performance. The optimum pH and molar ratio of the carrier to total metal ion content are 6.0 and 1.0, respectively [63]. There are two sharp and well-defined peaks in the cyclic voltammograms, revealing that $LiMn_2O_4$ particles are highly crystalline and intercalation–deintercalation processes occur at two stages in the 4 V region [64].

The enhancement in capacity in comparison with solid-state reactions can partly be ascribed to the smaller particles from sol-gel methods [55, 62], since the diffusion path for lithium ions is shorter and the change in the volume to surface area of individual particles during charge–discharge cycling is smaller [62]. The highly crystalline phase is the main cause [56, 58, 59].

$LiMn_2O_4$ can also be prepared directly from heating a gelatinous $LiMn_2O_4$ powder obtained by drying a sol from lithium acetate dihydrate, manganese acetate tetrahydrate and tartaric acid at 50 °C [65]. Amorphous and crystalline spinel materials can be obtained. It is found that the chemical diffusivity of lithium ions in the amorphous powder electrode specimen is nearly constant at about $10^{-8}$ $cm^2/s$, irrespective of the lithium content in the 0.45–0.7 range at room temperature, and 10 times higher than that in the crystalline material.

The improvement in electrochemical performance by sol-gel methods can be mainly ascribed to the marked decrease in disordering of $Li^{+}$ and $Mn^{3+}$ due to the low HTT and short heat-treatment time, short diffusion path from a small particle size, and the high-purity spinel phase of $LiMn_2O_4$.

In addition, sols can be used to prepare thin-film electrodes by spin coating and dip coating, which cannot be easily achieved by solid-state reactions [19].

## Doped lithium manganese oxides prepared by sol-gel methods

In order to circumvent the Jahn–Teller effect, the introduction of further heteroatoms is a preferable choice [2], such as Li, Al, Cr, Co, Ti, V or Ni.

Lithium doping produces $Li_{1+\delta}Mn_{2-\delta}O_4$ samples ($0.00 \le \delta \le 0.20$) by a sol-gel method, with good thermal stability [66, 67]. However, there is no discussion of the doping effects on electrochemical performance in this paper. Perhaps it is similar to lithium doping by other methods [2].

The Al-doped spinel $LiAl_xMn_{2-x}O_4$ ($x = 0.05, 0.15$) is synthesized by a sol-gel method using citric acid as the carrier. The effect of the calcination temperature on the purity of the Al-substituted spinel suggests that a pure material can be obtained by calcination at 800 °C. Al substitution enhances sintering of the spinel $LiMn_2O_4$ and improves substantially its capacity retention.

Doped spinels with the formula $LiM_{0.2}Mn_{1.8}O_4$ ($M = Cr$, Co) and $LiTi_{0.19}Mn_{1.76}O_4$ have been prepared using a sol-gel method involving $Mn(acac)_3$, $Cr(acac)_3$, $[Ti(acac)_3]_2[TiCl_6]$ and $Li_2CO_3$ as precursors and propionic acid as a carrier [69]. On firing at 600 °C, the gels turn into normal spinel phases of high purity. The Co- and Cr-doped spinels consist of very uniformly shaped microcrystals. The best performance is exhibited by the Co-doped spinel followed by the Cr-doped one, since they can depress capacity fading over 4 V owing to better ordering of the cations and structure stability [2, 35]. In contrast, $LiTi_{0.19}Mn_{1.76}O_4$ exhibits significant capacity fading upon cycling (3.2–4.6 V). All lithium in the Co- and Cr-doped manganese spinels can be extracted by charging the cells above 5 V. Under these conditions, only the Cr-doped spinel provides acceptable capacity retention upon cycling. The increased stability of $Cr^{4+}$ relative to $Mn^{4+}$ is the likely origin of the stabilization in the Cr-doped spinel structure under these drastic conditions [69]. A modified sol-gel method based on the carrier citric acid and nitrates can yield a Cr-doped spinel with good cyclability [70].

Nearly stoichiometric Li–V–Mn–O ternary spinels can also be prepared by a sol-gel method using propionic acid as the carrier to form a resin framework, followed by calcination of the gel at 600 °C [71]. V exists in an oxidation state of +5 and Mn in those of +3 and +4. During lithium intercalation and deintercalation the change in cation distribution is insignificant. The discharge–charge profiles of the resulting material are surprisingly similar to those reported for thin-film $LiMn_2O_4$ in the voltage range 5.2–2.0 V [1]. Although the spinel preserves its basic framework across the whole potential window, significant capacity fading is observed along the 5.0 and 2.0 V plateaus, which is associated with a reversible cubic–tetragonal phase transition. The best electrochemical performance of the cell has been observed in the potential window 4.6–2.5 V. Within this voltage range, the cell maintains an acceptable capacity (105 mAh/g) even after extensive cycling [71].

Spinel $LiMn_{1.95}Ni_{0.05}O_4$ powders with sub-micron, narrow size distribution and phase-pure particles are also synthesized by a sol-gel method [72]. Although the Ni-doped spinel has a smaller initial capacity of 126 mAh/g, it exhibits better cycling performance than the conventional one that delivers a higher initial capacity of 145 mAh/g. The improvement in cycling performance of the formed electrode is attributed to stabilization of the

spinel structure by the presence of nickel ions, low interfacial resistance and high lithium-ion diffusion [72].

The $Li^{+}/Co^{3+}$-codoped $LiMn_2O_4$ spinel has been prepared by a sol-gel method using citric acid as a carrier [73]. Since the manganese ions in the 16d sites are replaced by both lithium and cobalt ions, the obtained composition can be expressed with a new spinel formula, $(Li)[Mn^{3+}_{1-3x/2}Mn^{4+}_{1+x/2}Lix/4Co^{3+}_{3x/4}]O4$. The inclusion of lithium and cobalt ions in 16d sites enhances the electrochemical cyclability of $LiMn_2O_4$ at the expense of a slight decrease in the initial charge capacity. The improvement in cycling performance is mainly attributed to the suppression of Jahn–Teller distortion in the co-doped spinel [73].

The above results show that effective doping can result in improvement in electrochemical performance. Other kinds of cations can also be doped by sol-gel methods if they can produce favorable effects such as an increase in Mn valence to suppress the Jahn–Teller effect and an improvement in the stability of the spinel frame of $Li[Mn_2]O_4$ to lower or inhibit the structural change during charge and discharge processes and the Mn solution reaction happening as in Eq. 4. Heteroatoms producing unfavorable effects should be avoided for doping, such as a decrease in Mn valence promoting Jahn–Teller distortion, the formation of a heterogeneous phase as an impurity and destroying the uniformity of the spinel frame structure, and a decrease in the volume of the crystallite units of the spinel $Li[Mn_2]O_4$ to inhibit the movement of lithium. It should be pointed out that there is usually a trade-off between the cycle life and the capacity in the case of favorable doping.

Both cations and anions can be doped by sol-gel methods when their doping is very effective for improving the cycling performance of lithium batteries. The highly crystallized spinel oxysulfide $Li_{1.02}Mg_{0.1}Mn_{1.9}O_{3.99}S_{0.01}$ is synthesized by a sol-gel method using adipic acid as a carrier followed by heat treatment at 750 °C in an oxygen atmosphere [74]. Both Al and S can also be doped into $LiMn_2O_4$ by a sol-gel method using glycolic acid as a carrier [75, 76, 77]. Owing to the incorporation of both kinds of ions, which produce favorable effects [2], the structural stability during cycling is much improved, resulting in an increased cyclability [75]. The oxysulfide spinel $LiAl_{0.24}Mn_{1.76}O_{3.98}S_{0.02}$ prepared by a sol-gel method shows also excellent cycling behavior at high temperatures (50 and 80 °C) (Fig. 5). This results from a small structural degradation of the oxysulfide particle surface due to production of a rock salt, $Li_2MnO_3$, at the spinel surface [78, 79]. Nevertheless, its capacity also fades at a high temperature due to MnO dissolution of the formed $Li_2Mn_2O_4$ at the particle surface [80]. Another oxysulfide spinel, $LiCr_{0.19}Mn_{1.81}O_{3.98}S_{0.02}$, with a well-developed octahedral structure, is synthesized by a sol-gel method, also using glycolic acid as a carrier. It shows no capacity loss in the 3 V and 4 V regions since the substitution of S for O in $LiMn_2O_4$ stabilizes the structural integrity of the spinel host, which in turn increases the electrochemical cyclability [81].

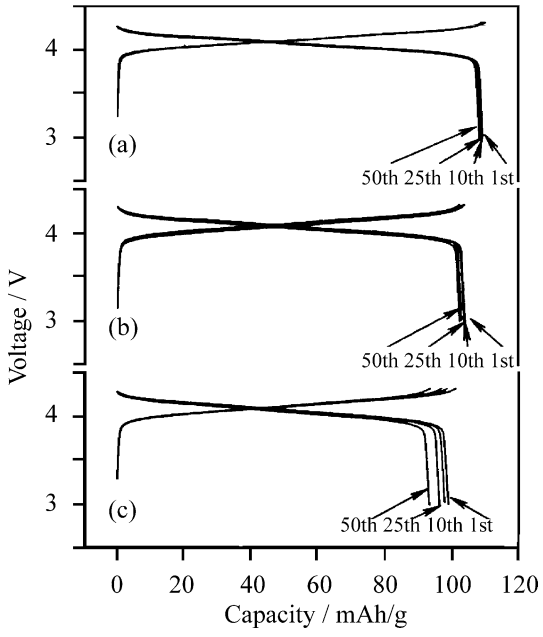


**Fig. 5** Charge–discharge curves of $LiAl_{0.24}Mn_{1.76}O_{3.98}S_{0.02}$ from a sol-gel method at (**a**) room temperature, (**b**) 50 °C and (**c**) 80 °C between 3 and 4 V as a function of cycle number, using lithium metal as counter and reference electrodes (from [79])

There is some dispute concerning doping with S. It was reported that S could not be doped into the spinel structure [82]. Perhaps it is calculated on the basis of a pure model. In fact, other kinds of anions can be doped, such as F and I [2]. In the case of I, the structure is changed. It could not be excluded that there is also some minor discrepancy in the structure of the S-doped spinel. From comparison of the charge–discharge curves of Fig. 4 and Fig. 5, some differences can be noted. Evidently, this needs further research to resolve the dispute.

Both Al- and Se-doped $LiMn_2O_4$ can be prepared by a sol-gel method using glycolic acid as a carrier [83]. $LiAl_{0.18}Se_{0.02}Mn_{1.8}O_4$ is a phase-pure polycrystalline material and shows two voltage plateaus at 3 V and 4 V. It delivers a discharge capacity of 81 and 178 mAh/g in the first cycle, which increases with cycling to reach 110 and 204 mAh/g after 50 cycles. The 4 V region is excellent in cycling and shows almost no capacity loss [83].

The oxygen-doped lithiated manganese oxide $Li_xMnO_{2+\delta}$ ($x$ is near 0.5), which is obtained via a sol-gel process to prepare an $\alpha$-$Na_{0.7}MnO_2$ crystalline phase, followed by an ion-exchange reaction with lithium and heat treatment, is a mixture of a spinel phase ($a = 8.16$ Å) and a lamellar phase [84]. Consequently, it is still included here. Its electrochemical performance is strongly dependent on the heat treatment of the Li-exchanged compound obtained after the ion-exchange procedure. The best results are obtained for the sample heat treated at 300 °C, and a stable capacity of 155 mAh/g is still achieved after 20 cycles performed at a C/20 rate [84].

Other kinds of anions can also be doped by sol-gel methods, but so far the main destination for doping has been aimed at the stabilization of the spinel structure

and/or the reduction of volumetric changes or stress from lithium intercalation.

### Coated lithium manganese oxides prepared by sol-gel methods

Like the coating of $LiCoO_2$ [24, 25] and $LiNiO_2$ [42], the surface of $LiMn_2O_4$ can also be coated with, for example, $LiCoO_2$ using a sol-gel method employing glycolic acid as a carrier. After coating, the rate capability and the cycling behavior at the high temperature (65 °C) of the obtained composite are much improved since Mn dissolution is suppressed and the thickness of the passivating film acting as an electronic insulating layer and the interparticle contact resistance are decreased [85, 86]. The main reason is that the $LiCoO_2$ coating has a higher conductivity ($10^{-2}$ S/cm) than that of $LiMn_2O_4$ ($10^{-6}$ S/cm). As a result, in the case of 7 mol% $LiCoO_2$-coated $LiMn_2O_4$, its reversible capacity is higher (120 mAh/g) than that of the as-received oxide (115 mAh/g), maintaining the same excellent cycling stability. The rate capability of $LiCoO_2$-coated $LiMn_2O_4$ improves significantly, and the reversible capacity increases by 60% at the 20 C rate (2400 mA/g) in comparison with that of the as-received one [86]. With respect to the nature of the coating, it has been reported that it is not $LiCoO_2$ but a newly formed spinel phase, $Li_{1+x}Mn_{2-x}Co_xO_4$, due to the heat treatment at 800 °C [87]. Consequently, the higher concentration of Co ions at the surface effectively protects the active material from $Mn^{2+}$ dissolution into the electrolytes, resulting in an improvement in the structural stability during cycling and in the electrochemical performance [87].

Other kinds of oxide can also be coated on the surface of $LiMn_2O_4$ by sol-gel methods, such as ZnO [88, 89, 90] and $LiAlO_2$ (actually in the form of $LiAl_xMn_{2-x}O_4$) [91]. In the case of $LiNi_{0.5}Mn_{1.5}O_4$ coated by ZnO, great improvements have been achieved [88, 89, 90]. It delivers an initial discharge capacity of 137 mAh/g with an excellent cyclability at the elevated temperature 55 °C, almost no capacity loss after 50 cycles, and maintains an almost perfect cubic spinel structure [88]. In contrast, $LiNi_{0.5}Mn_{1.5}O_4$ shows a serious capacity loss and exhibits a mixture of a tetragonal phase ($Li_2Mn_2O_4$), a rock salt phase ($Li_2MnO_3$) and a cubic phase ($LiMn_2O_4$) after 50 cycles at 55 °C. The main reason is that the small amount of the ZnO coating significantly reduces the content of HF or removes HF from the electrolyte [89]. Perhaps other factors, such as a suppression of the structural change, have also been in action.

These results show that the spinel $LiMn_2O_4$ prepared using sol-gel methods has a suitable arrangement of cations of $Mn^{3+}$, $Mn^{4+}$ and $Li^+$ in the crystal lattice, and thus distortion from the Jahn–Teller effect is slight and good cycling behavior is achieved. After doping, the stability of the spinel structure increases and not only is the Jahn–Teller effect alleviated but also the dissolution of $Mn^{2+}$ according to Eq. 4 is decreased. Consequently, the doped spinel shows excellent cycling, although there is a slight sacrifice of capacity. The coated spinel can achieve not only the above effects but also good rate capability and improved tolerance to overcharge and high temperature, due to the increase in conductivity among interparticles from the coating component [86] and the decrease in HF content in the electrolyte [89].

## Vanadium oxides

Vanadium is also cheap and easily derived from existing mineral deposits like Mn, and its oxides are attractive cathode materials due to the accommodation of three stable oxidation states ($V^{5+}$, $V^{4+}$ and $V^{3+}$) within their close-packed oxygen arrays. Among many structurally different vanadium oxides, layered vanadium pentoxides, $Li_xV_3O_8$, and their derivatives are promising cathode materials for lithium ion batteries since these kinds of structures can act as good hosts for the insertion and the reversible release of guest $Li^+$ ions. Vanadium in these compounds is pentavalent, and sol-gel method can be easily employed to prepare them.

### Vanadium pentoxides prepared by sol-gel methods

During the last two decades, many gel products of vanadium pentoxides have been prepared by sol-gel methods, such as hydrogels, xerogels, aerogels, bronzes and other oxides [1, 9, 92, 93, 94, 95, 96]. Hydrogels contain too much water and are not suitable as cathode materials for lithium ion batteries.

#### *Vanadium(V) oxides prepared by sol-gel methods*

Different precursors and different routes can result in markedly different structures, especially in the case of $V_2O_5$, leading to different electrochemical performance [97]. For example, the aqueous route via hydrolysis of vanadium oxide from vanadic acid usually leads to ordered gels with a layered structure, but the hydrolysis of alkoxide precursors results in an amorphous structure. As a result, there are some discrepancies between the experimental data.

Xerogels ($V_2O_5{\cdot}nH_2O$) are usually prepared from vanadic acid. They show a layered structure and there are trapped water molecules ($n$ can be as low as 0.5) [98]. They exhibit a very open microstructure, and ionic species can diffuse easily through the pores of the gel. They comprise flat ribbons and are characterized by a strong structural anisotropy corresponding to stacking in the same direction of the $V_2O_5$ ribbons. Owing to their cationic exchange properties in aqueous solution, a wide variety of exchanged xerogels can be obtained after removal of structural water at temperatures above 250 °C [98].

Film electrodes of xerogel can be easily obtained by coating a viscous gel on an indium tin oxide or stainless steel substrate [96, 99, 100]. In the cyclic voltammogram of the film oxide electrode dried at 130 °C, there are three different coupled reduction and oxidation current peaks corresponding to three kinds of distinctive intercalation sites for lithium [99]. In contrast, when it is dried at 270 °C, the xerogel is further dehydrated and the number of intercalation sites is reduced in the oxide film. As a result, only one current peak appears. The water molecules within the oxide xerogel film can change the xerogel oxide lattice to a more open-structured one and thereby more lithium ions can be absorbed into the oxide xerogel electrode. The lithium ion diffusion is mainly limited by the fractional number of vacant lithium intercalation sites since there is a drastic decrease in the chemical diffusivity of lithium ion after 2.4 V (vs. $Li^+/Li$) [99].

The thickness of the film electrode also determines the electrochemical performance of the $V_2O_5$ xerogel. When it is a thin-film electrode, an insertion of 4 $Li^+$/mol can be achieved, as shown in Eq. 5 [101, 102]:

$$4Li^+ + 4e^- + V_2O_5 \cdot 0.5H_2O \rightleftharpoons Li_4V_2O_5 \cdot 0.5H_2O \quad (5)$$

Its reversibility is good since it is a highly amorphous host structure and there is no permanent deformation or mechanical breakdown during the lithium insertion/deinsertion process. The specific energy can be 1300 mWh/g [102]. When it is a thick pellet electrode, its capacity is lower, $<2$ $Li^+$/mol [103]. The main reason is perhaps the limitation from its morphology or particle size, electronic conductivity or solid-state diffusivity [103].

Aerogel $V_2O_5$ can be obtained by conventional supercritical drying of the bulk liquid gel with liquid $CO_2$ [101]. Such a step can prevent the collapse of the network structure caused by surface tension forces. It is characterized by a bicontinuous structure of a solid phase and pores. The thickness of the solid phase surrounding the pores is in the range of 10–30 nm, which is also the diffusion distance for lithium intercalation into the solid phase. This solid diffusion distance is exceptionally short in comparison to most porous cathodes, from 1 to 100 μm. In addition, its surface area can be up to 450 $m^2/g$, much higher than that of a xerogel of a few square meters per gram. Moreover, the porous structure allows the electrolyte to penetrate deeply within the aerogel particles. As a result, aerogel $V_2O_5$ is good in rate capability. The cyclic voltammogram of the aerogel shows only one reversible pair of peaks around 3 V, while that of xerogel displays three pairs of current peaks. Almost 4 $Li^+$ per $V_2O_5$ aerogel can be inserted, as shown in Fig. 6a, and the voltage is stable at around 3 V. Consequently, in comparison with other kinds of $V_2O_5$ such as xerogels and amorphous ones, its specific energy is higher (Fig. 6b). The main reason is perhaps that the process of supercritical drying fundamentally changes the nature of the intercalation sites to yield better hosts for the Li insertion [101].

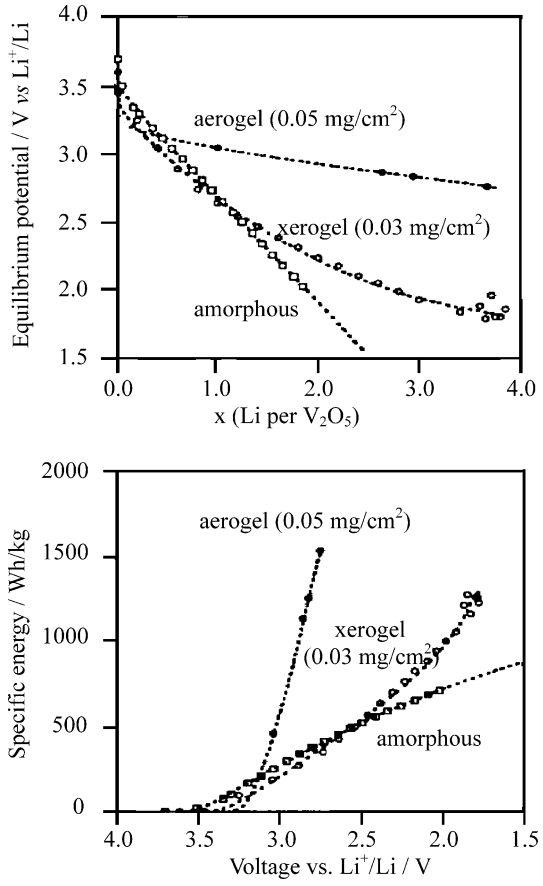


**Fig. 6** Equilibrium voltage–composition curves of a $V_2O_5$ aerogel (*top*) and its specific energy–equilibrium voltage curves (*bottom*) in comparison with xerogel and amorphous $V_2O_5$ (from [101])

α-$V_2O_5$ has a layered structure with a distorted close-packed oxygen array. Three lithium ions can be inserted, finally arriving at the composition $Li_3V_2O_5$. Crystalline α-$V_2O_5$ thin films can be prepared by the sol-gel route using vanadium oxo-isopropoxide as a precursor followed by annealing at a low temperature (400 °C) [104]. These films show different $Li_xV_2O_5$ phases from the $V_2O_5$ prepared by other techniques at high temperatures. For $x=0.0$ and $x=0.4$ the results are identical, and the phases are described as α-$V_2O_5$ ($x=0.0$) and ϵ-$Li_xV_2O_5$ ($x=0.4$). However, for a larger degree of intercalation some noticeable difference is apparent. First, the phase for $x=0.8$ shows an elongated $c$-axis compared to ϵ-$Li_xV_2O_5$ ($x=0.8$). Moreover, it is probably monoclinic. Secondly, the electrochemical and structural data do not provide any evidence for the formation of δ-$LiV_2O_5$ ($x=1.0$). Thirdly, the phase for $x=1.4$ bears some resemblance to δ-$LiV_2O_5$. The reason for these differences is sought in the structure and chemistry of these $V_2O_5$ films, which are different from those of a "standard" crystalline material owing to the low-temperature sol-gel preparation route, since the preparation procedure might be the cause of structural transitions and changes in lattice constants as well as of subtle changes in the chemical composition and the amount of stress [104].

In summary, there are various kinds of $V_2O_5$ gels prepared by sol-gel methods and the structure can also be different (crystalline or amorphous). These factors affect the electrochemical behavior considerably [96].

*Doped vanadium(V) oxides prepared by sol-gel methods*

Nevertheless, $V_2O_5$ prepared by normal sol-gel methods is still unsatisfactory since its capacity fades considerably. To improve its electrochemical performance, one possibility is to introduce heteroatoms such as iron, aluminum, chromium, copper or cesium during the sol-gel preparation to prepare bronzes [105, 106, 107, 108, 109, 110], like the doping of $LiMn_2O_4$ [2, 44]. Since xerogel consists of negatively charged ribbons and inter-ribbon protonated water, i.e. $(V_2O_{5.15})^{0.33-}(H_3O^+)_{0.33}(-H_2O)$, in this way, owing to its cationic exchange properties in aqueous solution, various ion exchanged xerogels can be obtained. Depending on the nature of cation species M, various bronzes (M = Na, K, Ag, Cu, Fe) or mixed oxides (M = Al) can be prepared by a subsequent appropriate heat treatment in air or other treatment [93, 96, 97, 105, 109]. The sodium bronze consists of very long platelets of 1–2 μm width that are arranged parallel to the *ab* plane, whereas packs of disordered particles of 2–10 μm size are observed for the bronze from solid-state reactions. Whatever the bronze compounds ($Na_{0.24}V_2O_5$, $Na_{0.33}V_2O_5$, $K_{0.25}V_2O_5$, $Ag_{0.33}V_2O_5$, $Ag_{0.4}V_2O_5$), their electrochemical behavior is generally characterized by three well-defined reversible insertion and deinsertion peaks at average potentials of 3.3, 2.9 and 2.55 V within the composition range of $0 < x \leq 0.33$–$0.4$, $0.35$–$0.4 < x \leq 0.7$–$0.75$ and $0.7$–$0.75 \leq x \leq 1.65$–$1.75$, respectively, which is better, at least by a factor of 2, than results obtained with the material from solid-state reactions.

In the doped $V_2O_5$, the dopant elements are distributed homogeneously in the prepared products and they increase interaction between $V_2O_5$ layers. For example, in the case of $Fe_{0.12}V_2O_5$, which resembles orthorhombic $V_2O_5$ in cell parameters, an introduced $Fe^{3+}$ ion locates between four oxygen atoms of the $V_2O_5$ slabs with additional oxygen atoms along the *c*-axis, above and below the iron site to complete the iron octahedral environment [105]. As to $Cr_{0.11}V_2O_{5.16}$ ($V_2O_5$-derived structure), the formed short $CrO_6$ octahedral chains link $V_2O_5$ layers to increase the three-dimensional stability [110]. In the case of the $Tb_{0.11}V_2O_5$ compound, the doped $Tb^{3+}$ ions bond with the rare-earth ions and the residual $H_2O$ in the $V_2O_5$ structure [111]. As a result, the stability of the layered structure increases during charge and discharge process and better cycling properties are achieved. For example, after 40 cycles in the voltage range 3.8–2 V (C/4) the reversible lithium capacity of $Fe_{0.12}V_2O_{5.16}$ can be still up to 200 mAh/g [105]. In the case of $Cr_{0.11}V_2O_{5.16}$, the reversible capacity can still be above 410 mAh/g after 40 cycles (Fig. 7).

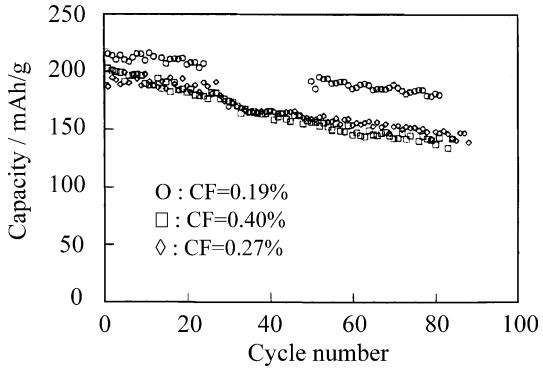


**Fig. 7** Cycling behavior of $Cr_{0.11}V_2O_{5.16}$ prepared by a sol-gel method. CF (capacity fading rate) = 100×capacity loss/(cycle number×initial capacity) (from [110])

In the case of Ag- and Cu-doped $V_2O_5$, up to 4 mol of lithium per mol of oxide can be reversibly intercalated [8, 109], and the composite cathodes also show excellent properties in terms of rate capability and very good reversibility upon cycling, with no capacity fading after more than 450 cycles, owing to the increase of electronic conductivity by two to three orders of magnitude and the consequent reversible high intercalation capability [97, 109, 112]. Lithiation of $Ag_xV_2O_5$ and $Cu_{0.1}V_2O_5$ bronze prepared from $V_2O_5$ hydrogels and metal powder proceeds with the concurrent formation of copper metal, and the starting parent compound can be regenerated upon removal of lithium, which is attributed to the excellent structural and electrochemical reversibility [97, 112].

In $Tb_{0.11}V_2O_5$, $Tb^{3+}$ ions are stable and are not involved in the oxidation–reduction during cycling [111]. The capacity fading is reduced, the specific reversible capacity is 330 mAh/g (C/4, cut-off 3.7–2.0 V) and there is a large voltage plateau at 2.5 V [111].

In comparison with those from solid-state reactions, the reversible capacity of bronzes from sol-gel methods is higher. For example, after 50 cycles a capacity of 120 mAh/g is still recovered, twice the capacity of that from solid-state reactions. The main cause is perhaps the higher diffusion coefficients of lithium, almost two orders of magnitude larger than with samples from solid-state reactions [96].

Oxides such as $RuO_2$ and $Na_2O$ units can also be doped into $V_2O_5$, which is different from the above-mentioned process [113, 114]. The doping with $RuO_2$ consists of three steps: (1) $V_2O_5$ hydrogels are prepared via protonation of sodium metavanadate solution followed by ion-exchange to obtain a homogeneous $V_2O_5$ hydrogel; (2) water in the hydrogel is exchanged with acetone, and then an organic solvent (hexane) with low surface tension is used to exchange acetone to prepare an organogel; (3) a $RuO_4$/hexane solution is added to the pre-cooled organogel, then the mixture is immersed in a dry-ice bath for 3 h before being transferred to a cooling bath (−22 °C) and kept there overnight. After final heating at 160 °C under air for 24 h,

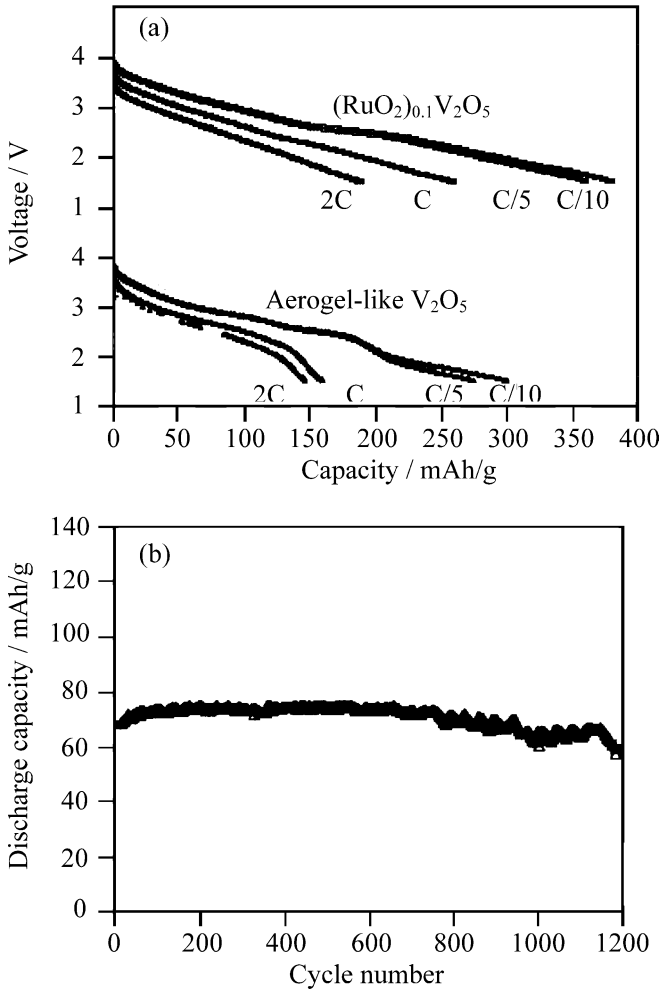


**Fig. 8** Electrochemical performance of $(RuO_2)_{0.1}V_2O_5$: (**a**) comparison of discharge curves of aerogel-like $V_2O_5$ and $(RuO_2)_{0.1}$-$V_2O_5$ at different rates; (**b**) cycling behavior of $(RuO_2)_{0.1}V_2O_5$ at a 5 C discharge rate (from [113])

$(RuO_2)_{0.1}V_2O_5$ is obtained [113]. Its conductivity increases sharply, $10^4$ times than that of pure aerogel-like $V_2O_5$. This route preserves the free volume of the aerogel and it can support a high rate of intercalation, as shown in Fig. 8a. Its reversible capacity can be up to 400 mAh/g at C/10 and good cycling behavior over 1200 cycles is achieved (Fig. 8b) [113]. $(Na_2O)_{0.23}V_2O_5$ is synthesized by precipitation of a sol to obtain a precipitate of $(Na_2O)_{0.23}V_2O_5{\cdot}xH_2O$, which can lose water at 200 °C. After removal of the water at a temperature below 250 °C, the prepared quasi-tetragonal crystallite $(Na_2O)_{0.23}V_2O_5$ is in platelet form, and its dimension is less than 2 μm. Its behavior is different from that of the above bronzes and the reversible capacity can be more than 220 mAh/g in 12 cycles when the voltage is from 3.8 to 1.8 V. Since its synthesis is relatively easy, in comparison with other forms of vanadium oxide, its electrochemical performance is satisfactory [114].

In summary, the doped elements in $V_2O_5$ act as pillars between the vanadium oxide layers and thus stabilize the structure during intercalation and deintercalation, providing good cycling behavior. In addition, the atoms between the interlayers increase the interlayer distance and therefore more electroactive species can be inserted, resulting in high reversible capacity. Moreover, these pillars increase the diffusion rate of lithium ions in the materials, and improve the kinetics of the charge and discharge reactions as potential cathode materials for high rate capability.

### *Vanadium(V) oxides prepared by modified sol-gel methods*

The reviewed sol-gel methods can also be modified to prepare $V_2O_5$ [1, 115, 116]. The lithium capacity of $V_2O_5$ from traditional methods is limited, and is less than 2 Li/mol. When the size of the $V_2O_5$ from the sol-gel method is controlled to be in the nanometer range, the intercalation of lithium can be up to 5.8 molar [1]. This great increase in capacity can be ascribed to two factors: the sites for lithium intercalation are changed and thermodynamically better sites for lithium intercalation are produced. In addition, the interlayer distance between $V_2O_5$ sheets increases, resulting in a nearly two-dimensional ordered structure; the interaction between the sheets is weak, and thus lithium can intercalate more easily [1].

When surfactants are added during the preparation process to modify the sol-gel method, they slow down the gelling rate during the hydrolysis process. After obtaining a gel, they are removed and the porosity is increased significantly; the $Li^+$ diffusion coefficient is 100 times higher than those of materials from traditional methods [115]. As a result, a high rate capability is possible.

Supercritical drying of a hydrogel can also be modified to prepare an organogel of $V_2O_5$ [116]. Water in the initially prepared sodium metavanadate hydrogel is substituted with acetone instead of supercritical drying. Then cyclohexane is used to substitute acetone to obtain an organogel [116]. The organic solvent cyclohexane in the organogel is removed during drying to prepare the electrode material. Although there might be some remaining organic solvent, this will not cause irreversible capacity because it is inert [116].

A template-based sol-gel method can be employed to prepare nanorolls of $V_2O_5$ using triisopropyloxyvanadium(V) oxide, $[(CH_3)_2CHO]_3VO$, as precursor and hexadecylamine ($C_{16}H_{33}NH_2$) and dodecylamine ($C_{12}H_{25}NH_2$) as templating molecules. The nanorolls consist of several layers of $V_2O_5$ with an outer diameter of 15–100 nm, an inner diameter of 5–50 nm and a length up to 15 μm. The interlayer distance of the 001 planes increases significantly, even in comparison with that of cation-substituted vanadium oxide [117].

A membrane-based template sol-gel method can also be used to prepare nanostructured $V_2O_5$ by hydrolyzing triisopropoxyvanadium(V) oxide to form a gel and deposit within the pores of a polymer membrane. Chemical

etching can be used to change both the pore diameter and porosity of the membrane. After formation of the gel $V_2O_5$, the organic membrane is removed and the resulting electrodes consist of $V_2O_5$ nanofibrils like the bristles of a brush [118].

A modified sol-gel method can also be utilized to prepare nanotubes of $V_2O_5$ through hydrolysis of triisopropoxyvanadium(V) oxide in the presence of the structurally directing hexadecyclamine and subsequent hydrothermal treatment [119]. This tube consists of several concentric shells, each about 2.8–3 nm in thickness. The external diameter of the tube is between 15 and 100 nm, and the internal one between 5 and 50 nm [119].

The above modified sol-gel methods can yield various kinds of vanadium oxides, especially with novel nano characteristics, and their electrochemical performance depends on the preparation methods. In the case of the $V_2O_5$ nanoroll, its reversible capacity is only up to 200 mAh/g, but good cycling can be achieved [117]. An organogel of $V_2O_5$ presents a high reversible capacity of 410 mAh/g and a capacity fading rate as low as 0.19% per cycle owing to the formation of a stable porous structure [116]. The obtained $V_2O_5$ nanofibril shows good volumetric and geometric rate capabilities, even higher than that of a comparable thin-film electrode [118]. However, the capacity of a $V_2O_5$ nanotube fades fast with the cycle number [119]. It is certain that their different electrochemical performance is related to the change of structure derived from the preparation methods. So far, there is still no systematic exploration of this topic.

With the development of sol-gel methods in combination with other technology, new kinds of vanadium oxides will be explored and the current ones will win an improvement in their electrochemical performance as cathode materials.

### Layered $LiV_3O_8$ and its derivatives

Layered $LiV_3O_8$ has a monoclinic symmetry (space group $P2_1/m$) and can be regarded as a lithia-stabilized $V_2O_5$ compound. It consists of octahedral [$VO_6$] and trigonal bipyramidal [$VO_5$] ribbons. In this structure, distorted [$VO_6$] octahedral sites are connected via shared edges and vertices to form $[V_3O_8]^-$ strands that are stacked one upon another to form quasi layers. On lithiation up to the composition of $Li_4V_3O_8$, the $V_3O_8$ framework remains intact and there is no change in the unit cell volume, although the monoclinic unit cell parameters vary isotropically and it undergoes several phase changes. Owing to the stability of the $V_3O_8$ sublattice and the availability of a two-dimensional interstitial space for lithium-ion transport, $LiV_3O_8$ is an attractive cathode candidate for lithium ion batteries [1]. When it is obtained in a finely dispersed form by dehydration of aqueous lithium vanadium gels followed by drying and heat treatment to remove loosely bound water, it shows higher reversible capacity, almost 4 $Li^+$/mol, with better cycling than that of crystalline $LiV_3O_8$ from solid-state reactions [120], mainly because the material is directly prepared with a small particle size and short, unblocked diffusion paths during the sol-gel process.

$NaV_3O_8$ has the same monoclinic structure as $LiV_3O_8$ and can be considered as being one of its derivatives. Sodium ions are situated between quasi layers. In this way, the positively charged sodium ions electrostatically hold together the $[V_3O_8]^-$ strands. The spacing between the strands is also sufficiently flexible to accommodate other guest species on octahedral and tetrahedral interstitial sites. It can also be prepared by the sol-gel method, which, in this case, is also called the precipitation method [121]. Lithium can intercalate chemically and electrochemically therein. In the case of the former, up to 3 $Li^+$/mol could be inserted in the water-free lattice, and about 2.5 $Li^+$/mol can be deinserted in the potential range 1.5–4.0 V, corresponding to a specific capacity of about 250 mAh/g. In the case of the latter, almost 3.5 $Li^+$/mol could be inserted, and a specific reversible capacity of more than 200 mAh/g can be attained for 100 cycles, independent of the applied current up to 50 mA/g of the oxide, indicating good rate capability [121].

$LiV_3O_8$ and its derivative from sol-gel methods show good electrochemical performance due to its stable layered structure. In addition, they have fast insertion–deinsertion kinetics and high reversible capacity. Consequently, its application will not be far away if a discharge profile as stable as that of an aerogel can be maintained [101].

## Other cathode materials

Other cathode materials mainly include $CrO_3$, $MoO_3$ and ferrous phosphates [1]. As ferrous phosphates are the most promising, only they are reviewed here.

$LiFePO_4$ is a type of ferrous phosphate and has long been regarded as a cathode material that cannot be charged and discharged at a high rate [1]. Using ascorbic acid as a carrier for a sol-gel method in combination with a reducing agent, a low concentration (1 wt%) of metals such as copper and silver is added to prepare metal-dispersed $LiFePO_4$ [122]. This metal addition does not affect the structure of the cathode but considerably improves its kinetics in terms of capacity delivery and cycle life owing to a reduction in the particle size and an increase in the bulk intra- and interparticle electronic conductivity from the finely dispersed metal powders. The improved conductivity favors the response of $LiFePO_4$, thus substantiating the interest in it as a new promising cathode material for lithium ion batteries [122]. Other kinds of organic carriers can be used, but those having a benzyl structure are preferred, because the residual carbon can act efficiently to enhance the electronic conductivity, leading to an improved electrochemical performance [123].

Moreover, when ferrous phosphate is prepared via a sol-gel route by adding phosphate ions to a solution of $Fe^{2+}$ and then heating in air at 100 °C [124], an amorphous compound of $3Fe_2O_3{\cdot}2P_2O_5{\cdot}10H_2O$ consisting of $FePO_4$ and $Fe_2O_3$ phases is obtained. During lithium intercalation, all the iron in $FePO_4$ is in the +2 oxidation state while that in $Fe_2O_3$ remains in the +3 oxidation state. Its capacity can be up to 140 mAh/g at 25 mA/g. Its specific capacity is not very sensitive to the discharge rate. When the discharge current increases tenfold, the utilization decreases only to about 76%. More then 1000 cycles can be achieved at about 50% of depth of discharge [124].

Since Fe-based cathode materials are environmentally compatible and simple in processing, and $LiFePO_4$ has good thermal stability in comparison with $LiCoO_2$, $LiNiO_2$ and $LiMn_2O_4$ [125], the ferrous phosphates will provide a promise for lithium ion batteries to be used as power sources for electric vehicles.

## Conclusions

In summary, sol-gel methods are important to improve the electrochemical properties of cathode materials for lithium ion batteries. In the case of lithium cobalt oxides, not only the reversible capacity and the cycling behavior are improved, but also the cost is lowered by doping and the tolerance to overcharge is increased by coating.

With lithium nickel oxides, layered compounds with a high phase purity can be easily obtained by a low heat-treatment temperature to overcome the reduction of $Ni^{4+}$ and disordering of $Li^+$ and $Ni^{3+}$, and the structural stability during cycling is increased by doping with heteroatoms and coating. As a result, the reversible capacity is enhanced, the cycling behavior is improved, and the overcharge ability is increased, resulting in a promising candidate for industrial application.

With spinel-type lithium manganese oxides, the degree of disordering of the cation distribution in the crystal lattice is greatly circumvented due to good mixing; the Jahn–Teller effect is alleviated. In addition, the stability of the spinel structure is increased and dissolution of $Mn^{2+}$ is decreased owing to effective doping and coating. Consequently, the cycling behavior is greatly improved. After coating, the rate capability is also improved.

Various compounds based on vanadium(V) oxide can be prepared, and their capacity, rate capability and cycling stability are greatly improved by doping and modification of sol-gel methods.

With the development of sol-gel methods in combination with other technologies, new and better cathode materials with unique properties may become available, such as inorganic-organic nanocomposite cathode materials [126, 127, 128, 129, 130], novel layered $LiM_xMn_{1-x}O_2$ (M = single or multi metal elements) withimproved cycling [131, 132, 133, 134, 135] and 5 V cathode materials. The practical application of Fe-based cathode materials will be realized in the near future.

Moreover, one main advantage of the sol-gel methods is the possibility to prepare nanomaterials, which become more and more important in science and technology. In the near future, a lot of nano cathode materials will be prepared, and microbatteries will come into use for application in microelectronic devices such as microsatellites, providing promising applications for cathode materials prepared by sol-gel methods [4].

**Acknowledgements** Financial support from the Alexander von Humboldt Foundation and the China Natural Science Foundation (20333040) is greatly appreciated. Thanks are due to S. Bach, G. Fey, A. Manthiram, E.A. Menlenkamp, J. Morales, H.B. Park, D.M. Schleich, Y.K. Sun and M.M. Thackeray for kindly supplying reprints.

## References

1. Wu YP, Wan C, Jiang C, Fang SB (2002) Lithium ion secondary batteries. Chemical Industry Press, Beijing
2. Wu YP, Rahm E, Holze R (2002) Electrochim Acta 47:3491
3. Wu YP, Rahm E, Holze R (2003) Chin J Power Sources 27:45
4. Wu YP, Rahm E, Holze R (2002) Chin J Batteries (Dianchi) 32:256
5. Manthiram A, Kim J (1999) Recent Res Dev Electrochem 2:31
6. Manthiram A, Kim J (1998) Chem Mater 10:2895
7. Wu YP, Rahm E, Holze R (2003) Chin J Power Sources 27:45
8. Klein L (1988) Sol-gel technology. Noyes, Park Ridge, USA
9. Brinker CJ, Scherer GW (1990) Sol-gel science. Academic Press, San Diego, USA
10. Livage J, Henry M, Sanchze C (1989) Prog Solid State Chem 18:259
11. Wu YP, Wan C, Jiang C, Li J, Li Y (2000) Chin J Power Sources 24:112
12. Yoshio M, Tanaka H, Tominaga K, Noguchi H (1992) J Power Sources 40:347
13. Kanga SG, Kang SY, Ryu KS, Chang SH (1999) Solid State Ionics 120:155
14. Yoon WS, Kim KB (1999) J Power Sources 81–82:517
15. Sun YK, Oh IH, Hong SA (1996) J Mater Sci 31:3617
16. Sun YK (1999) J Power Sources 83:223
17. Jeong E, Won M, Shim Y (1998) J Power Sources 70:70
18. Alcantara R, Lavela P, Tirado JL, Stoyanova R, Kuzmanova E, Zhecheva E (1997) Chem Mater 9:2145
19. Rho YH, Kanamura K, Umegaki T (2003) J Electrochem Soc 150:A107
20. Peng Z, Wan C, Jiang C (1998) J Power Sources 72:215
21. Zhou YK, Shen CM, Li HL (2002) Solid State Ionics 146:81
22. Yoon W, Lee K, Kim K (2001) Electrochem Solid-State Lett 4:A35
23. Yoon WS, Lee KK, Kim KB (2001) J Power Sources 97–98:303
24. Cho J, Kim YJ, Park B (2001) J Electrochem Soc 148:A1110
25. Cho J, Kim CS, Yoo S (2000) Electrochem Solid-State Lett 3:362
26. Choi YM, Pyun SI, Moon SZ, Hyung YE (1998) J Power Sources 72:83
27. Song MY, Lee R (2002) J Power Sources 111:97
28. Lee YS, Sun YK, Nahm KS (1999) Solid State Ionics 118:159
29. Kweon HJ, Kim SS, Kim GB, Park DG (2002) J Mater Sci Lett 17:1697
30. Sun YK, Oh IH (1997) J Mater Sci Lett 10:30
31. Cho J, Kim G, Lim H (1999) J Electrochem Soc 146:3571

32. Park S, Park K, Sun Y, Nahm K, Lee Y, Yoshio M (2001) Electrochim Acta 46:1215
33. Fey G, Shiu RF, Subramanian V, Chen JG, Chen CL (2002) J Power Sources 103:265
34. Liu H, Li J, Zhang Z, Gong Z, Yang Y (2003) J Solid State Electrochem 7:456
35. Zhecheva E, Stoyanova R, Alcantara R, Lavela P, Tirado JL (2002) Pure Appl Chem 74:1885
36. Fey G, Subramanian V, Chen JG (2001) Electrochem Commun 3:234
37. Hwang BJ, Santhanam R, Chen CH (2003) J Power Sources 114:244
38. Song MY, Lee R, Kwon I (2003) Solid State Ionics 156:319
39. Kweon HJ, Kim GB, Lim HS, Nam SS, Park DG (1999) J Power Sources 83:84
40. Chang CC, Kumta PN (1998) J Power Sources 75:44
41. Fey G, Subramanian V, Chen JG (2002) Mater Lett 52:197
42. Cho J, Kim TJ, Kim YJ, Park B (2001) Electrochem Solid-State Lett 4:A159
43. Thackeray MM (1997) Prog Solid State Chem 25:1
44. Wu YP, Li Y, Wan C, Jiang C (2000) Chin J Funct Mater 31:18
45. Thackery MM (1995) J Electrochem Soc 142:2558
46. Thackeray MM (1995) Prog Batt Batt Mater 14:1
47. Gummow RJ, Kock A, Thackeray MM (1994) Solid State Ionics 69:59
48. Jang D, Shin YJ, Oh SM (1996) J Electrochem Soc 143:2204
49. Aurbach D, Levi MD, Gamulski K, Markovsky B, Salitra G, Levi E, Heider U, Heider L, Oesten R (1999) J Power Sources 81–82:472
50. Guyomard D, Tarascon JM (1992) J Electrochem Soc 139:937
51. Guyomard D, Tarascon JM (1994) Solid State Ionics 69:222
52. Park YJ, Kim JG, Kim MK, Chung HT, Kim G (2000) Solid State Ionics 130:203
53. Liu W, Farringto GC, Chaput F, Dunn B (1996) J Electrochem Soc 143:879
54. Wang X, Chen XY, Gao LS, Zheng HG, Ji MR, Shen T, Zhang ZD (2003) J Crystal Growth 256:123
55. Park HB, Hong YS, Yi JE, Kweon HJ, Kim SJ (1997) Bull Korean Chem Soc 18:612.
56. Sun YK, Oh IH, Kim KY (1997) Ind Eng Chem Res 36:4839
57. Lee YS, Sun YK, Nahm KS (1998) Solid State Ionics 109:285
58. Sun YK (1997) Solid State Ionics 100:115
59. Sun YK, Lee KH, Moon SI, Oh IH (1998) Solid State Ionics 112:237
60. Prabaharan S, Saparil N, Michael S, Massot M, Julien C (1998) Solid State Ionics 112:25
61. Yang W, Liu Q, Qiu W, Lu S, Yang L (1999) Solid State Ionics 121:79
62. Guan J, Liu ML (1998) Solid State Ionics 110:21
63. Hwang BJ, Santhanam R, Liu DG (2001) J Power Sources 101:86
64. Hwang BJ, Santhanam R, Liu DG (2001) J Power Sources 97–98:443
65. Pyun SI, Choi YM, Jeng ID (1997) J Power Sources 68:593
66. Dziembaj R, Molenda M, Majda D, Walas S (2003) Solid State Ionics 157:81
67. Dziembaj R, Molenda M (2003) J Power Sources 119–121:121
68. Hwang BJ, Santhanam R, Liu DG, Tsai YW (2001) J Power Sources 102:326
69. Hernan L, Morales J, Sanchez L, Santos J (1999) Solid State Ionics 118:179
70. Du K, Xie J, Wang J, Zhang H (2003) J Power Sources 119–121:130
71. Hernan L, Morales J, Sanchez L, Santos J, Castellon ER (2000) Solid State Ionics 133:179
72. Sun YK, Kim DW, Choi Y (1999) J Power Sources 79:231
73. Hong YS, Han CH, Kim K, Kwon CW, Campet G, Choy JH (2001) Solid State Ionics 139:75
74. Park SH, Park KS, Moon SS, Sun YK, Nahm KS (2001) J Power Sources 92:244
75. Sun YK, Oh B, Lee HJ (2000) Electrochim Acta 46:541
76. Sun YK, Jeon YS (1999) Electrochem Commun 1:597
77. Sun YK (2000) Electrochem Commun 2:6
78. Sun YK, Jeon YS, Lee HJ (2000) Electrochem Solid-State Lett 3:7
79. Sun YK, Park GS, Lee YS, Yoashio M, Nahm LS (2001) J Electrochem Soc 148:A994
80. Sun YK (2001) Electrochem Commun 3:199
81. Sun YK, Oh IH (2001) J Power Sources 94:132
82. Goodenough JB (1998) In: Wakihara M, Yamamoto O (eds) Lithium ion batteries: fundamentals and performance. Wiley-VCH, Weinheim, Germany
83. Sun YK (2001) J Appl Electrochem 31:1149
84. Franger S, Bach S, Pereira-Ramos JP, Baffierb N (2001) J Power Sources 97–98:344
85. Park SC, Han YS, Kang YS, Lee PS, Ahn S, Lee HM, Lee JY (2001) J Electrochem Soc 148:A680
86. Park SC, Kim YM, Kang YM, Kim KT, Lee PS, Lee JY (2001) J Power Sources 103:86
87. Cho J, Kim GB, Lim HS, Kim CS, Yoo SI (1999) Electrochem Solid-State Lett 2:607
88. Sun YK, Lee YS, Yoshio M, Amine K (2002) Electrochem Solid-State Lett 5:A99
89. Sun YK, Hong KJ, Prakash J, Amine K (2002) Electrochem Commun 4:344
90. Amatucci G, Tarascon JM (2002) J Electrochem Soc 149:K31
91. Sun YC, Wang ZX, Chen LQ, Huang XJ (2003) J Electrochem Soc 150:A1294
92. Livage J (1991) Chem Mater 3:578
93. Pereira-Ramos JP (1995) J Power Sources 54:120
94. Zaralij PZ, Whittingham MS (1999) Acta Crystallogr Sect B 55:627
95. Rolison DR, Dunn B (2001) J Mater Chem 11:963
96. Livage J (1996) Solid State Ionics 86–88:935
97. Coustier F, Passerini S, Smyrl WH (1997) Solid State Ionics 100:247
98. Park HK, Smyrl WH, Ward MD (1995) J Electrochem Soc 142:1068
99. Pyun SI, Bae JS (1997) J Power Sources 68:669
100. Vinod MP, Bahnemann D (2002) J Solid State Electrochem 6:498
101. Le DB, Passerini S, Chu X, Chang D, Owens BB, Smyrl WH (1995) In: Megahed S, Barnet BM, Xie L (eds) Rechargeable lithium and lithium ion batteries. The Electrochemical Society, Pennington, NJ, USA, p 306
102. Passerini S, Le DB, Foong HC, Owens BB, Smyrl WH (1995) In: Megahed S, Barnet BM, Xie L (eds) Rechargeable lithium and lithium ion batteries. The Electrochemical Society, Pennington, NJ, USA, p 297
103. Tipton A, Passerini S, Owens BB, Smyrl WH (1996) J Electrochem Soc 143:3473
104. Meulenkamp EA, Klinken W, Schlatmann AR (1999) Solid State Ionics 126:235
105. Gregoire G, Soudan P, Farcy J, Pereira-Ramos J, Badot J, Baffier N (1999) J Power Sources 81–82:612
106. Baddour-Hadjean R, Farry J, Pereiar-Ramos JP (1996) J Electrochem Soc 143:2083
107. Maingot S, Deniard PH, Baffier N, Pereira-Ramos JP, Kahn-Harari A, Brec R, Willmann P (1995) J Power Sources 54:342
108. Coustier F, Jarero G, Passerini S, Smyrl WH (1999) J Power Sources 83:9
109. Coustier F, Hill J, Owens BB, Passerini S, Smyrl WH (1999) J Electrochem Soc 146:1355
110. Soudan P, Pereira-Ramos JP, Farcy J, Gregoire G, Baffier N (2000) Solid State Ionics 135:291
111. Almeida EC, Abbate M, Rosolen JM (2002) J Power Sources 112:290
112. Giorgetti M, Mukerjee S, Passerini S, McBreen J, Smyrl WH (2001) J Electrochem Soc 148:A768
113. Zhang F, Paserini S, Owens BB, Smyrl WH (2001) Electrochem Solid-State Lett 4:A221
114. Dai J, Li S, Gao Z, Siow K (1998) J Power Sources 74:40

115. Mege S, Routhier D, Ansart F, Savarianst JM (1998) Mol Cryst Liq Cryst Sci Technol Sect A 311:503
116. Couster F, Passerini S, Smyrl WH (1998) J Electrochem Soc 145:L73
117. Nordlinder S, Edstroem K, Gustafsson T (2001) Electrochem Solid-State Lett 4:A129
118. Patrissi CJ, Martin CR (2001) J Electrochem Soc 148:A1247
119. Spahr ME, Stoschitzki-Bitterli P, Nesper R, Haas O, Novak P (1999) J Electrochem Soc 146:2780
120. West K, Zachau-Christiansen B, Skaarup S, Saidi Y, Barker J, Olsen II, Pynenburg R, Koksbang R (1996) J Electrochem Soc 143:820
121. Spahr ME, Novak P, Scheifele W, Haas O, Nesper R (1998) J Electrochem Soc 145:421
122. Croce F, D'Epifanio A, Hassoun J, Deptula A, Olczac T, Scrosati B (2002) Electrochem Solid-State Lett 5:A47
123. Doeff MM, Hu YQ, McLarnon F, Kostecki R (2003) Electrochem Solid-State Lett 6:A207
124. Prosini P, Cianchi L, Spina G, Lisi M, Scaccia S, Carewska M, Minarini C, Pasquali M (2001) J Electrochem Soc 148:A1125
125. Wu YP, Dai XB, Ma JQ, Chen YJ (2004) Lithium ion batteries: applications and practices. Chemical Industry Press, Beijing
126. Goward GR, Leroux F, Nazar LF (1998) Electrochim Acta 43:1307
127. Shouji E, Buttry DA (1999) In: Abstracts, 8th international meeting on macromolecule-metal complexes, Tokyo, Japan, p 49
128. Huguenin F, Giz M, Ticianelli E, Torresi R (2001) J Power Sources 103:113
129. Neves S, Fonsec C (2002) J Power Sources 107:13
130. Park SK, Lee YS, Sun YK (2003) Electrochem Commun 5:124
131. Park SH, Sun YK (2003) J Power Sources 119–121:161
132. Kim JH, Sun YK (2003) J Power Sources 119–121:166
133. Guo ZP, Konstantinov K, Wang GX, Liu HK, Dou SX (2003) J Power Sources 119–121:221
134. Kang SH, Sun YK, Amine K (2003) Electrochem Solid-State Lett 6:A183
135. Kim JH, Yoon CS, Sun YK (2003) J Electrochem Soc 150:A538